

Estimation of ion adsorption using iterative analytical model in capacitive deionization process

Muhammad Shafiq^a, Karthik Laxman^b, Joydeep Dutta^{b,*}

^aDepartment of Electrical and Computer Engineering, College of Engineering, Sultan Qaboos, University, PO Box 33, Al-Khoudh, Muscat – 123, Sultanate of Oman, email: mshafiq@squ.edu.om (M. Shafiq)

^bFunctional Materials, Applied Physics Department, SCI School, KTH Royal Institute of Technology, Isafjordsgatan 22, SE-16440 Kista Stockholm, Sweden, email: laxman@kth.se (K. Laxman), Tel. +46-73-765 21 86, email: joydeep@kth.se (J. Dutta)

Received 27 September 2017; Accepted 3 April 2018

ABSTRACT

Capacitive deionization (CDI) is an upcoming technique that can replace existing processes for removing and recuperating metal ions from dilute industrial waste waters. CDI removes ions via electrosorption on to its electrode surfaces, the efficiency of which is a function of CDI electrode properties that progressively change during continued operation. As such a need exists to develop a model to predict CDI performance over elongated periods which is independent of electrode properties and has negligible error values. By applying a first order non-linear dynamic model (FONDM) with inputs independent of the electrode characteristics, we propose a universal model that can predict CDI ion adsorption capacity with changes in applied potential, flow rate and electrolyte temperature to within 5% of the experimentally obtained results. The model was verified using activated carbon cloth (ACC) as a test electrode and aqueous sodium chloride solution as electrolyte, with a good prediction for ion electrosorption efficiency and time dependent electrosorption dynamics. The simplicity of the model makes it easy to adapt for various applications and in the development of intelligent control systems for CDI units in practical settings.

Keywords: Activated carbon cloth; Analytical model; Ion adsorption; Capacitive deionization (CDI); Electrosorption

1. Introduction

Manufacturing industries produce a large quantity of metal ion contaminated wastewater that can pollute the environment [1]. Industrial processes like adsorption, ion exchange and chemical precipitation are often used for the removal of hazardous elements, but small amounts of metal ions are difficult to remove by these classical processes. Particularly the recovery of heavy metal ions from dilute solutions is considered to be a key problem, requiring commercially viable solutions to circumvent ion concentration processes prior to its removal [2]. Capacitive deionization (CDI) is a plausible solution which works by electro-adsorption of water borne charged species (ions) on electri-

cally polarized electrodes at low applied potentials [3–10]. As electrosorption capacity is proportional to the surface area of the electrodes taking part in the ion adsorption process, activated carbon based materials are the primary choice for CDI electrodes [11–16]. Besides the electrode surface area, water temperature, flow rate, ion concentration etc., affect the ion electrosorption capacity [17,18], making CDI efficiency estimation models important to save time and cost. CDI models are typically developed on the principle of an electric double layer (EDL) formation at the electrode-electrolyte (water) interfaces [19], theory of which has been established through the classical reports of Helmholtz, Gouy, Chapman, Stern, Debye, Hückel and others [20]. Modified Donnan model (mD) [21,22] is one such model which uses electrode thickness, pore distribution, chemical and electronic charge etc., to estimate ion adsorption capacity and dynamics with changes in ion concentration and

*Corresponding author.

applied potential [23–27]. Other modeling techniques have relied on Poisson's and Nernst-Planck equations [28] or differential equations (with and without analytical solutions) [25,29,30] to successfully model CDI behavior taking into account electrode and device parameters like cell resistance, columbic efficiency, capacitance etc. [31–33].

In this work, we have developed an analytical model based on CDI device performance to predict the time dependent ion adsorption capacity for a CDI device, independent of the physical, chemical or electronic properties of the device or the electrode. The method is verified for CDI device constructed with activated carbon cloth and sodium chloride (NaCl) as a test electrode solution respectively. Due to its independence of device and electrode variables, the present model will be particularly useful for upscaling and designing field operational CDI systems.

2. Model

2.1. Prior considerations

A typical conductivity curve obtained from the CDI device used for this work, illustrating the operational regimes (adsorption/desorption) of a CDI process is shown in Fig. 1. For this experiment, the CDI unit is switched to desorption mode after the point of minimum conductivity is reached, for energy efficient CDI operation [34]. The model focuses on the period prior to the minimum conductivity point (at which the process is quasi-stable for a brief period), which corresponds to the maximum ion adsorption rate, subsequent to which the energy efficiency of the ion-removal process decreases rapidly. Using this period the model builds up an analytical solution to dynamically predict the conductivity value prior to and at the quasi-stable state of CDI operation.

2.2. Model development

A closer look at Fig. 1 indicates that the rate of change of conductivity of the CDI cells at time 't+x' depends on the

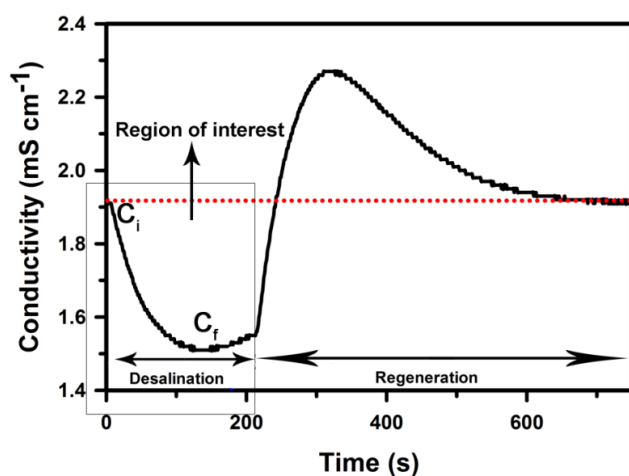


Fig. 1. Typical conductivity curve of a continuous flow between CDI cell showing the desalination and regeneration regions.

initial value at ($t = 0$) and the value at time 't'. Thus a linear system identification technique based on step responses is applied to develop first order and second order linear dynamic models for the system. In these models, the over-damped response is approximated by a first order stable linear dynamic system and the under-damped response by the second order stable linear dynamic system [35,36]. The conductivity response in the adsorption region illustrated in (Fig. 1) can be represented by an over-damped linear dynamic system with an output that has an additive portion of the input [4,5]. For the CDI cell, the input variables considered for the model are electrical conductivity (at time 't'), voltage (volts), temperature ($^{\circ}\text{C}$) and volume flow rate (mL/min) which are an additive part of the conductivity (at time ($t + x$)) and the output variable of interest is the electrical conductivity during electrosorption. Thus the CDI cell step response is represented by:

$$C(t) = C_0 + KP(1 - e^{-\alpha(t)t}) \quad (1)$$

The impulse response of the above equation can be given by,

$$\dot{C}(t) = -a(t)(C(t) - C_0) + a(t)KP \quad (2)$$

where $C(t)$ represents the conductivity as a function of time t , P is one of the input variables, $C_0 = C(t_0)$ is the initial value of conductivity, $\dot{C}(t) = \frac{dC(t)}{dt}$ is the time derivative of $C(t)$, K , $\alpha(t)$ and $a(t)$ are the unknown CDI cell parameters. The impulse response Eq. (2) is introduced to obtain the time varying dynamic model of the CDI system. This model also approximates the nonlinear behavior of the unknown variables.

During ion adsorption, electrical conductivity behavior suggests that $\alpha(t) > 0$. Intuitively, $\alpha(t)$ should be a time dependent function of all the variables represented by P . However, this would lead to computational difficulties in the identification process. Therefore, to develop a simple algorithm for estimating the unknown parameters, we assigned $\alpha(t)$ as a polynomial of order n , i.e.

$$\alpha(t) = \sum_{j=0}^p \alpha_j t^j \quad (3)$$

and

$$a(t) = \frac{d\alpha(t)t}{dt} = \sum_{k=0}^p (j+1)\alpha_j t^j \quad (4)$$

where p and j represent positive integers and p is the order of the polynomial $\alpha(t)$ and $a(t)$. The motivation behind the choice is that most of the static bound continuous functions can be approximated by the polynomials [37]. The polynomial $\alpha(t)$ captures the effects of unknown variables in the CDI system that can cause variation in the dynamic behavior of the system. It is important to note that the identification of polynomial $\alpha(t)$ does not need measurement of the variables like surface area, porosity, roughness, pore path arrangement etc. The effect of these variables cumulatively appears in the conductivity output of the CDI device.

It can be observed that Eq. (1) is the solution of the nonlinear dynamic Eq. (2) upon inserting the value of $C(t)$ in Eq.

(2). This leads to reducing the problem of simple estimation of the unknown parameters K and α_j .

2.3. Estimation of unknown parameters (K and α_j)

Let us consider \hat{K} , $\hat{\alpha}(t)$ and $\hat{a}(t)$ as the estimates of K , $\alpha(t)$ and $a(t)$. It is presumed that the data is collected over a uniform sampling period ΔT and, where, ΔT satisfies the Shanon criterion. The sampled time instance t_k is given by $t_k = k\Delta T$, where k is a positive integer. Thus the following relationship can be used for the prediction of the conductivity at any discrete instance t_k following the equation as given below:

$$C(t_k) = C_0 + \hat{K}P(1 - e^{-\hat{\alpha}(t_k)t_k}) \tag{5}$$

If we assume that column vector $C = [C_0, C_1, \dots, C_n]^T$ is the data of the electrical conductivity at constant sampling time instance t_k , C can be acquired by computer data acquisition system as $C_k \approx C(t_k)$. It is also reasonable to consider that some of the data in the vector C belongs to the steady state region (minimum outlet conductivity) of the electro-sorption region. The average of the steady state region thus can be expressed by C_e

$$C_e = \frac{1}{n - i + 1} \sum_{k=i}^n C_k \tag{6}$$

where C_e represents the estimate of the theoretical final value C_F (i.e. $C_F \approx C_e$), C_i is the measured steady state value. All the values of C_k in $C_s = [C_i, C_{i+1}, \dots, C_n]$ are in the vicinity of C_F (i.e. $C_k = C_e + e_k$), e_k represents measurement noise in the steady state and C_F is defined by,

$$C_F = \lim_{t \rightarrow \infty} C(t) = \lim_{t \rightarrow \infty} (C_0 + KP(1 - e^{-\alpha(t)t})) = C_0 + KP \tag{7}$$

The parameter \hat{K} can thus be obtained using Eq. (7) and definition of C_e

$$K \approx \hat{K} = \frac{C_e - C_0}{P} \tag{8}$$

In order to obtain $\alpha(t)$ polynomial, we perform algebraic operations on Eqs. (5) and (8) to derive,

$$\hat{\alpha}(t_k) = \frac{\ln\left(\frac{C(t_k) - C_e}{C_0 - C_e}\right)}{t_k} \tag{9}$$

Using $C_k \approx C(t_k)$, $\alpha(t_k)$ can be given by

$$\alpha(t_k) \approx \frac{\ln\left(\frac{C_k - C_e}{C_0 - C_e}\right)}{t_k} \tag{10}$$

Using Eq. (10), the column vector $\alpha = [\alpha(t_0), \alpha(t_1), \dots, \alpha(t_n)]^T$ can be easily computed. Let us define, $\hat{\alpha} = [\hat{\alpha}(t_0), \hat{\alpha}(t_1), \dots, \hat{\alpha}(t_n)]^T$ and an error vector, $e = \hat{\alpha} - \alpha$. The $e(t_k) = \sum_{j=0}^p \alpha_j t_k^j$ is the k^{th} element of vector $\hat{\alpha}$. Then, we consider an error function $\phi(\hat{\alpha}_0, \hat{\alpha}_1, \dots, \hat{\alpha}_p) = 0.5e^T e$.

Therefore, if the error vector follows the normal probability distribution, then the minimization of $\phi(\hat{\alpha}_0, \hat{\alpha}_1, \dots, \hat{\alpha}_p)$ yields p linear independent equations, called normal equations. These normal equations can be written in the matrix form as $A^T A \hat{\alpha} = A^T \alpha$. Where, matrix is given by,

$$A = \begin{bmatrix} t_0^0 & t_0^1 & \dots & t_0^{p-1} & t_0^p \\ t_1^0 & t_1^1 & \dots & t_1^{p-1} & t_1^p \\ \vdots & \vdots & \ddots & \vdots & \vdots \\ t_n^0 & t_n^1 & \dots & t_n^{p-1} & t_n^p \end{bmatrix}$$

The solution of these normal equations is a vector

$$\hat{\alpha} = [\hat{\alpha}_0, \hat{\alpha}_1, \dots, \hat{\alpha}_p]^T = (A^T A)^{-1} A^T \alpha \tag{11}$$

The elements of this vector are the estimates of the coefficients of the polynomial $\alpha(t)$. This estimation process is referred to as l_2 approximation or norm2 estimation [37]. The selection of the degree p of the polynomial $\hat{\alpha}(t)$ is an important iterative process. A mean square error δa , acceptable to the performance of CDI cell is used to determine p . The mean square error can then be defined by:

$$\delta = \frac{1}{n + 1} \sum_{k=0}^n (C_k - C(t_k))^2 \tag{12}$$

Once the parameter $\hat{\alpha}(t)$ is determined, then the estimate of $\alpha(t)$ can be obtained using Eq. (4) as

$$\hat{a}(t) = \frac{d\hat{\alpha}(t)t}{dt} = \sum_{k=0}^p (j+1) \hat{\alpha}_j t^j \tag{13}$$

The flow chart of the algorithm is given below in Fig. 2:

3. Experimental

The capacitive deionization (CDI) cell was fabricated by sandwiching a pair of ACC electrodes between two acrylic supports (10 mm thickness each). A spacer medium comprising of two layers of cellulose with pore dimensions around 25 μm and an approximate thickness of $\sim 500 \mu\text{m}$ (for two layers) was inserted between the carbon electrodes (Fig. 3).

FM-100 activated carbon cloth (ACC) from Zorflex with an average thickness of 1.0 mm and a BET specific surface area of about 1200 m^2/g [38,39] was used as CDI electrodes. All ACC samples were cleaned with hot 2 M nitric acid (HNO_3) at 115°C for 12 h following which the samples were thoroughly rinsed with deionized water and dried. The activated carbon cloth (ACC) used for the electrodes have a total pore volume of 1.42 $\text{cm}^3 \text{g}^{-1}$; of which 0.56 $\text{cm}^3 \text{g}^{-1}$ is comprised of micropores, 0.86 $\text{cm}^3 \text{g}^{-1}$ of macropores and 0.001 $\text{cm}^3 \text{g}^{-1}$ of mesopores. Graphite plates and rods for current collection and potential application are contacted with the ACC electrodes via holes drilled in the acrylic. The ACC electrodes were 8.5 cm^2 each, giving a total electrode area of $\sim 17 \text{cm}^2$ (2 electrodes) per CDI cell.

Ion-adsorption studies with different applied voltages were conducted on equilibrated ACC electrodes using the flow through CDI cell described above. The experiments were carried out with 1 g L^{-1} sodium chloride (NaCl) solution in DI water at flow rates ranging from 2 mL min^{-1} to 5 mL min^{-1} , and DC potentials ranging from $1.6 \text{ V}_{\text{DC}}$ to $3.0 \text{ V}_{\text{DC}}$. Heidolph pump drive 5201 was used to control the flow rate. For temperature dependent measurements, saline feed temperature was measured and controlled at the input of the CDI cell. Real time conductivity data was recorded

using eDAQ ET916 online conductivity probe with a cell volume of $93 \mu\text{l}$, coupled to a single channel conductivity isopod (EPU357). Desalination efficiency (DSE %) is calculated as follows:

$$DSE(\%) = \frac{C_0 - C_f}{C_0} \times 100 \quad (14)$$

where C_0 and C_f are the initial and final conductivity of saline (NaCl) solution

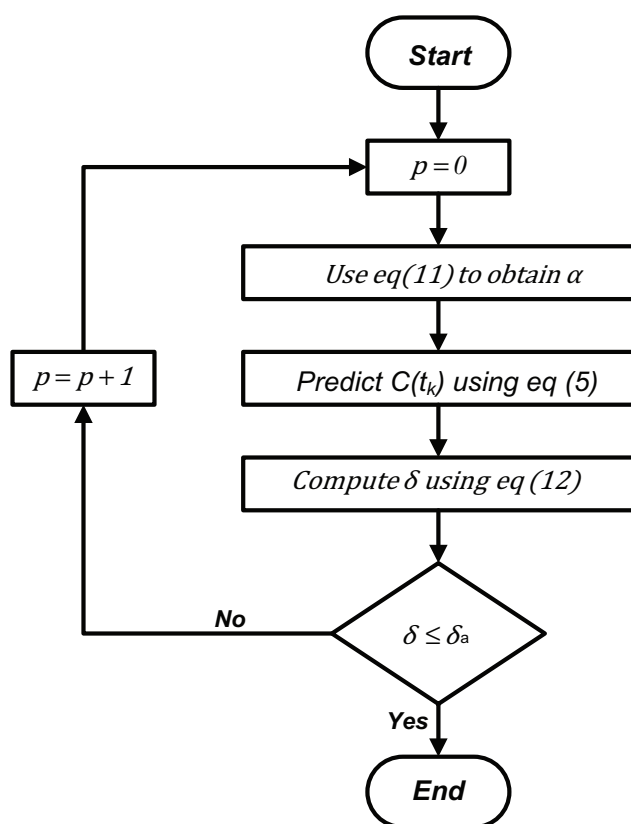


Fig. 2. Flow chart.

4. Results

4.1. Desalination results

To demonstrate the suitability of the nonlinear dynamic model, we extract the experimental conductivity data from the CDI system with different applied potentials, flow rates and temperatures as shown in Fig. 4. Desalination efficiency (DSE) increases quasi-linearly with applied cell potential up to 3.0 VDC as shown in Fig. 4a. The electrolysis of water which reduces charge efficiency, occurs at 1.23 V (against a standard hydrogen electrode), typically limiting the operating potential to $1.2\text{--}1.5 \text{ VDC}$ [5,40,41]. However, the upper limit of cell potential is a function of the material induced over potential (additional energy required for electrolysis), which in the case of ACC is ascertained to be 1.6 VDC based on the pH measurements (Fig. 4a). Below the applied voltage of 1.6 VDC , pH changes are negligible, while beyond this value a significant change is observed, attributed to water electrolysis and other complex reactions taking place at the electrode surfaces. However for practical purposes 1.6 VDC is chosen as the upper level of applied potential.

At a constant cell potential of 1.6 VDC , increased electrolyte flow rate led to linear decrease in the DSE of the CDI cell, from 50% at 1 mL min^{-1} to 10% at 5 mL min^{-1} (Fig. 4b), attributed to the effect of two simultaneous ion transport forces existing within the CDI cell. The first acts perpendicular to the electrode surface and is an integral function of the concentration gradient induced ion diffusion and the cell potential governed electro migration of the ions. The second acts tangentially (convective) to move the ion laterally across the electrode surface and is proportional to the

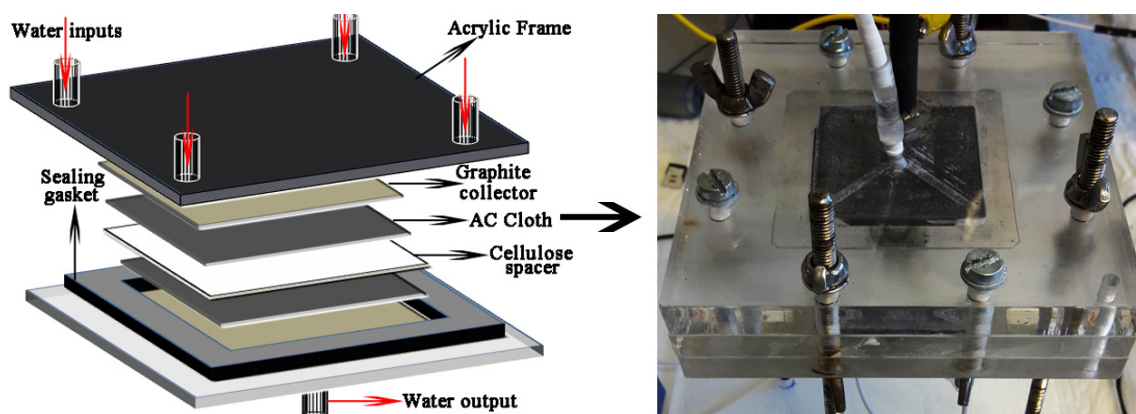


Fig. 3. On the left is a schematic illustration of the CDI cell structure used for the experiments. AC stands for activated carbon. On the right is an image of the CDI cell.

electrolyte flow rate. Upon increasing the flow rate, the tangential transport component of the ion movement increases, reducing the time available for ion adsorption to give a corresponding decrease in the desalting efficiency (Fig. 4b).

Desalination efficiency displays a more complex nature with changes in the electrolyte temperature. Typically, the efficiency is inversely proportional to the thickness of the

electrical double layer, which in turn is proportional to the electrolyte temperature. Thus an increase in temperature of the electrolyte leads to a reduction in the DSE. However, the results in Fig. 4c indicate that the desalination efficiency initially increases with temperature up to $\sim 50^\circ\text{C}$, beyond which a decrease is observed. The decrease at higher temperatures is as per the equations governing the electrical double layer principles, but the initial increase in DSE is unexpected.

While no obvious reasons for this trend can be established, it is hypothesized that electrolyte viscosity and mobility of the ions are responsible for these changes. Migration of ions to the respective electrodes (upon applying a cell potential) is accompanied by friction in the opposite direction due to solvent viscosity. Considering Stokes' expression which relates friction force ' F ' and viscosity of electrolyte ' η ' ($F = 6\pi\eta rv$ for ions with radius ' r ' and velocity ' v '), it can be observed that the friction force decreases with a decrease in electrolyte viscosity. Typically for water, the viscosity changes from 1.138 cP at 15°C to 0.379 at 75°C (at $25^\circ\text{C} = 0.890$ and $50^\circ\text{C} = 0.547$ cP); almost 50% reduction in viscosity at 50°C when compared to room temperature (25°C). The reduced viscosity also increases ion mobility and promotes improved access to the predominantly microporous ACC surface for ion adsorption, possibly explaining the initial increase in desalting efficiency with temperature. However a further increase in temperature widens the electrical double layer (EDL) thickness, leading to a reduction of the amount of ions stored in the EDL and hence the associated desalination efficiency. Thus the response of a CDI cell is a balance between increased ion adsorption due to viscosity and mobility and decrease due to EDL widening. Below 50°C the former has a greater effect than the latter, leading to increase in desalination efficiency, while above 50°C the wider EDL leads to a net reduction in the DSE.

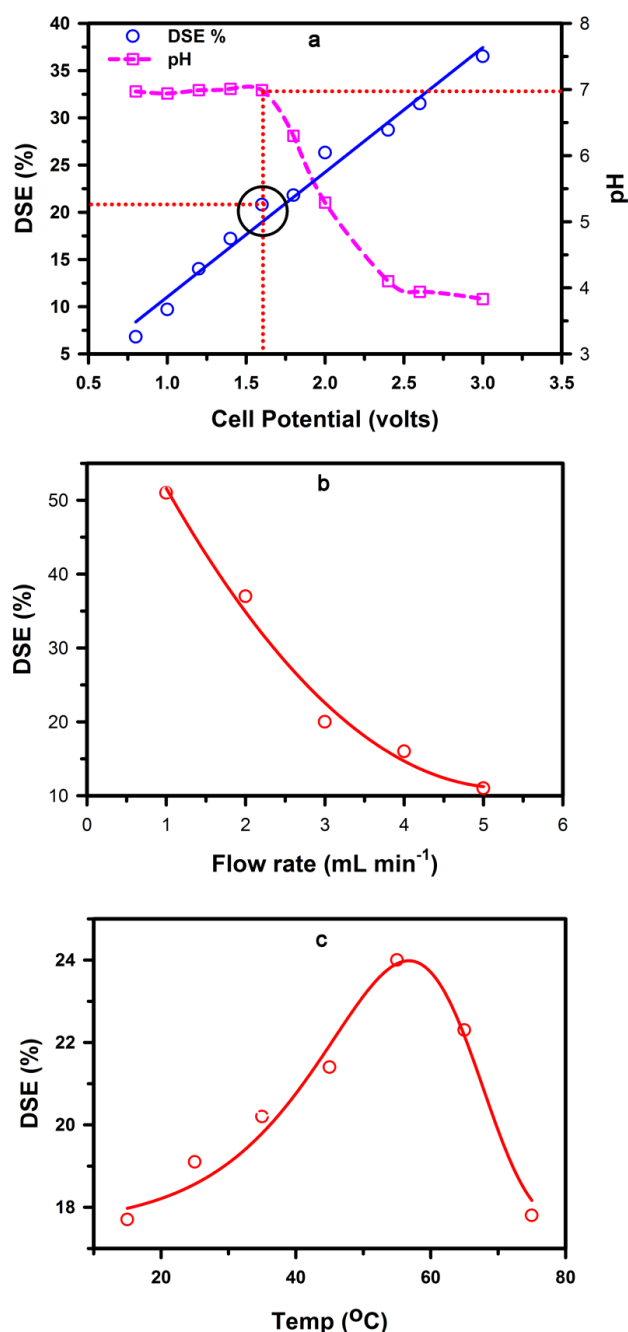


Fig. 4. Experimental results of desalting efficiency (DSE) and rate with changes in (a) cell potential; (b) flow rate of electrolyte and (c) temperature of electrolyte in degree Celsius. All experiments are performed using a 1 g L^{-1} NaCl electrolyte in DI water. Lines serve to guide the eye.

4.2. Verification of the model

The model parameters (K and $\alpha(t)$) are extracted from the individual conductivity plots plotted for various input parameter combinations (Figs. 5a, 6a and 7a). To improve model accuracy, the % absolute error is set to a maximum of 5% for all the cases. The estimated values of constant ' K ' and time dependent nonlinear parameter ' $\alpha(t)$ ' are listed in Table 1.

Using model 1, the magnitude and rate of change of ionic conductivity for applied potentials of 1.2 V and 0.8 V are predicted (based on equation parameters from the experimental points obtained for CDI process using 1.6 V) as shown in Figs. 5b and 5c. The predicted values are within 3% of the experimentally recorded ionic conductivities obtained for the applied potentials of 0.8 and 1.2 V.

The increase in error % with deviation from the potential at which ' K ' and ' $\alpha(t)$ ' are deduced (1.6 VDC) can be understood by analyzing the correlation of the model parameters to the CDI process. Typically a change in applied potential results in a change of the electrode capacitance and charge efficiency. In the model, these changes are represented by the constant ' K ', which is the coefficient for potential dependent capacitance and charge efficiency of the process, along with the time dependent non-linear function ' $\alpha(t)$ ', which is the coefficient for potential dependent ion adsorption rate.

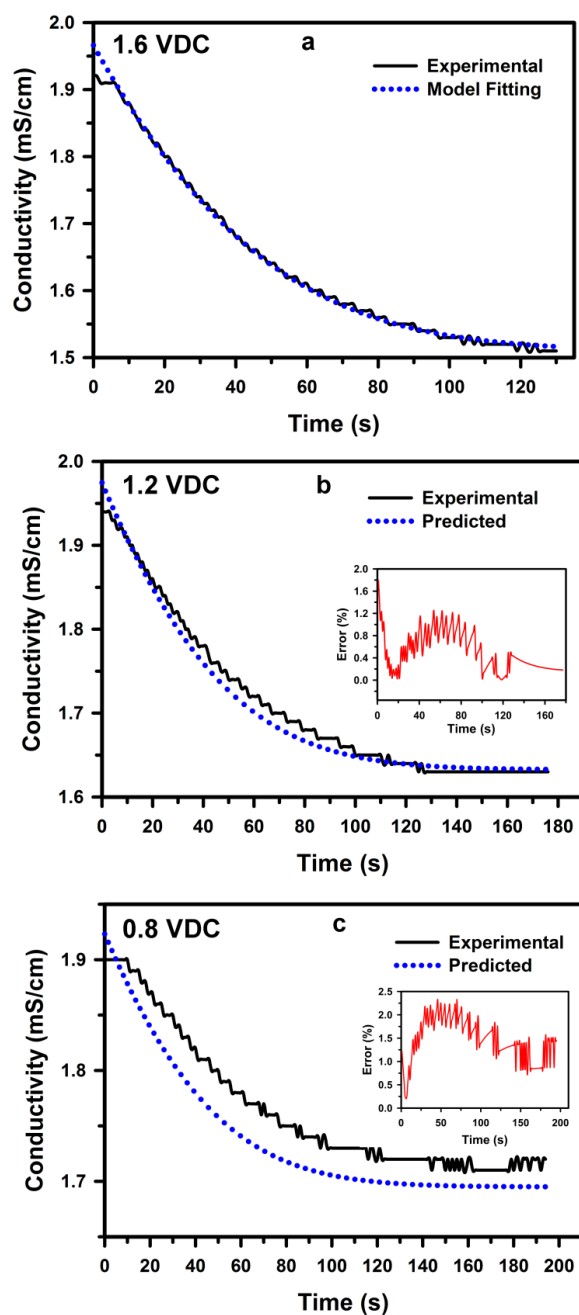


Fig. 5. Experimental and math model predicted conductivity trends for applied potential magnitudes of (a) 1.6 VDC; (b) 1.2 VDC and (c) 0.8 VDC. The parameter values were extracted from the experimental conductivity curve at 1.6 VDC and subsequently used to predict the desalting trends at 1.2 VDC and 0.8 VDC. Experiments were conducted at 25°C at a flow rate of 3 mL min⁻¹.

As both the total salt adsorption capacity and rate are over estimated for 0.8 VDC, it appears that the surface charge density and hence ' K ' is over estimated, which also results in over estimation of the initial ion adsorption rate represented by ' $\alpha(t)$ '. This could possibly explain the minor increase in error % as the value of applied potential deviates further from the point at which (' K ' and ' α ') were ini-

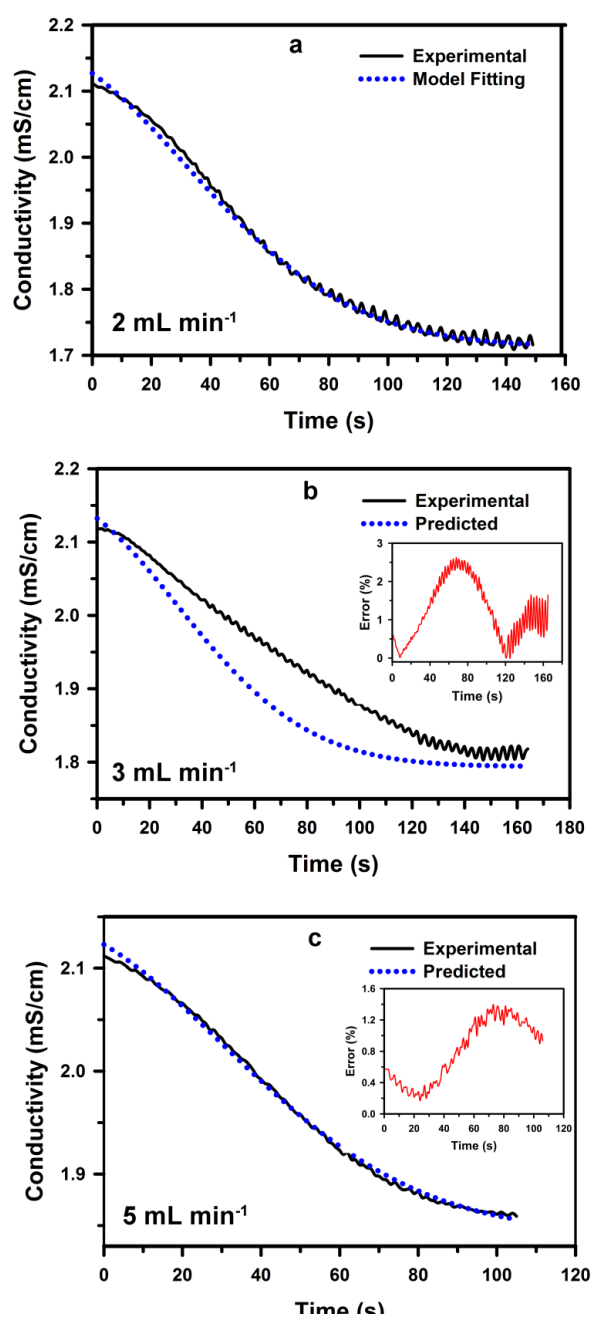


Fig. 6. Experimental and math model predicted conductivity trends for electrolyte flow rates of (a) 2 mL min⁻¹; (b) 3 mL min⁻¹ and (c) 5 mL min⁻¹. The parameter values were extracted from the experimental conductivity curve at 2 mL min⁻¹ and subsequently used to predict the desalting trends at 3 mL min⁻¹ and 5 mL min⁻¹. Experiments were conducted at 25°C at an applied potential of 1.6 VDC.

tially extracted. Nonetheless even with a 50% change in the applied potential, the maximum error % is only 2.0%, suggesting that the model is perfectly applicable for potential ranges viable for CDI operation.

Similarly, model 2 was used to predict changes in conductivity trends for flow rates of 3 mL min⁻¹ and 5 mL min⁻¹ (Figs. 6b and 6c), respectively, and model 3 to predict

conductivity trends at an electrolyte temperature of 50°C (Fig. 7b). The error percentages for the predicted values lie well within the set limits of 5% range (< 4% in all cases) providing a good approximation of the recorded experimental data. The discrepancy observed for 3 mL min⁻¹ can be possibly explained due to over estimation of the initial rate at which ions move toward the electrode surface (' α '), while the capacitance represented by (' K ') is correctly predicted as observed by the quasi steady state conductivity. Since these values correlate well with the predicted conductivity curve

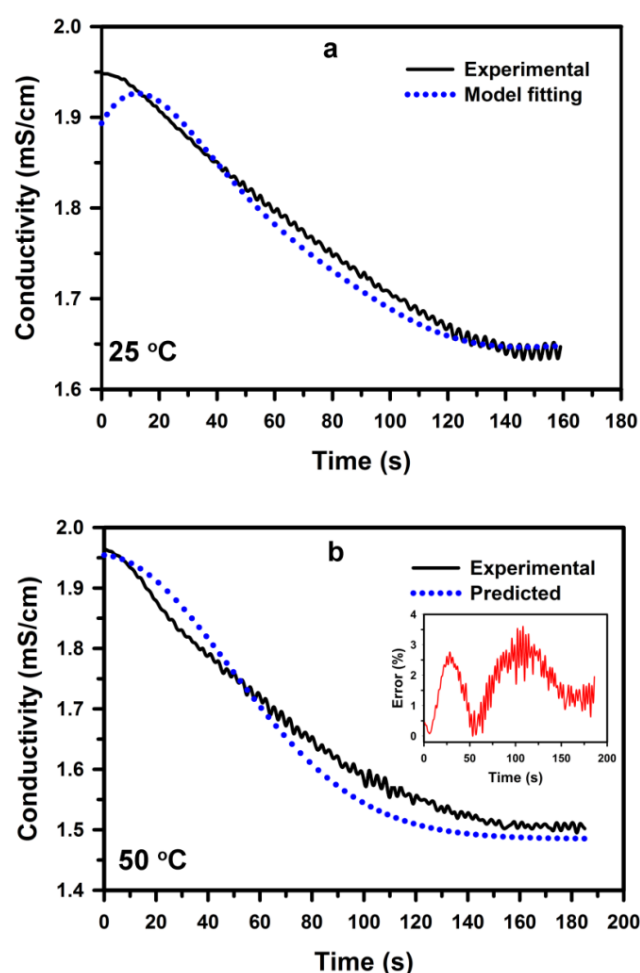


Fig. 7. Experimental and math model predicted conductivity trends for electrolyte temperatures of (a) 25°C and (b) 50°C. The parameter values were extracted from the experimental conductivity curve at 2°C and subsequently used to predict the desalting trends at 50°C. Experiments were conducted at a flow rate of 3 mL min⁻¹ and an applied potential of 1.6 VDC.

at 5 mL min⁻¹, it appears that there are exchanges that occur at the electrode-water interface at 3 mL min⁻¹ which presently cannot be explained. It is also to be noted that for conductivity trends for variations in electrolyte temperature, the model was used to predict desalination efficiency with temperatures varying from 15°C to ~50°C. Beyond 50°C, the salt removal trend reverses and thus new ' K ' and ' α ' values would need to be identified for this regime, before predicting the desalination efficiency for higher temperatures.

Hence by incorporating a simple curve fitting technique, an accurate and applicable mathematical equation to predict changes in ion adsorption trends with respect to changes in the applied potential, flow rate and electrolyte temperature are obtained. This method is a simpler approach to extracting not only the ion adsorption efficiencies as has been achieved by models reported in the literature [29–32], but also generates a good dynamic approximation of the adsorption rates which can be very helpful in setting the optimal operational point of an existing system.

5. Conclusion

In conclusion, an analytical model to describe the transient adsorption behavior of a CDI device is developed and verified. The model extracts its arguments from the ionic conductivity curve during the ion removal process and predicts the time dependent ion adsorption dynamics and capacity of an activated carbon cloth (ACC) electrode with changes in the applied potential, flow rate and electrolyte temperature with negligible errors. It is found that the ion-adsorption efficiency is directly proportional to applied potential, inversely proportional to flow rate of the electrolyte and has a complex nature with temperature with a trend reversal at 50°C. The experimental and theoretical results confirm the validity of the model and possible future applications in predicting the performance of CDI systems.

Acknowledgments

MS would like to thank Sultan Qaboos University for financial assistance. KL and JD would like to thank KTH Royal Institute of Technology.

References

- [1] M.A. Barakat, New trends in removing heavy metals from industrial wastewater, *Arab. J. Chem.*, 4 (2011) 361–377.
- [2] K. Tamaoki, N. Saito, T. Nomura, Y. Konishi, Microbial recovery of rhodium from dilute solutions by the metal ion-reducing bacterium *Shewanella* algae, *Hydrometallurgy*, 139 (2013) 26–29.

Table 1
Numerical value of constant ' K ' and time dependent nonlinear parameter ' $\alpha(t)$ '

| Model | Parameter | K | $\alpha(t)$ | Closed form model |
|-------|-------------------------------------|---------|--------------------------------|---|
| 1 | Potential (1.6 V) | -0.2562 | $0.001t^2 + 0.0206t - 0.1279$ | $C(t) = C_0 + KP(1 - e^{-\alpha(t)t})$ |
| 2 | Flow rate (2 mL min ⁻¹) | -0.4 | $0.0002t^2 + 0.0076t - 0.0479$ | $C(t) = C_0 + (K/F)(1 - e^{-\alpha(t)t})$ |
| 3 | Temperature (25°C) | -0.0120 | $0.0002t^2 + 0.0003 - 0.0217$ | $C(t) = C_0 + KT(1 - e^{-\alpha(t)t})$ |

- [3] J. Li, X. Wang, H. Wang, S. Wang, T. Hayat, A. Alsaedi, X. Wang, Functionalization of biomass carbonaceous aerogels and their application as electrode materials for electro-enhanced recovery of metal ions, *Environ. Sci.: Nano*, 4 (2017) 1114–1123.
- [4] S. Porada, R. Zhao, A. van der Wal, V. Presser, P.M. Biesheuvel, Review on the science and technology of water desalination by capacitive deionization, *Prog. Mater. Sci.*, 58 (2013) 1388–1442.
- [5] M.E. Suss, S. Porada, X. Sun, P.M. Biesheuvel, J. Yoon, V. Presser, Water desalination via capacitive deionization: what is it and what can we expect from it?, *Energy. Environ. Sci.*, 8 (2015) 2296–2319.
- [6] K. Laxman, M.T.Z. Myint, M. Al Abri, P. Sathe, S. Dobretsov, J. Dutta, Desalination and disinfection of inland brackish ground water in a capacitive deionization cell using nanoporous activated carbon cloth electrodes, *Desalination*, 362 (2015) 126–132.
- [7] I. Cohen, E. Avraham, Y. Bouhadana, A. Soffer, D. Aurbach, The effect of the flow-regime, reversal of polarization, and oxygen on the long term stability in capacitive de-ionization processes, *Electrochim. Acta*, 153 (2015) 106–114.
- [8] X. Gao, A. Omosibi, J. Landon, K. Liu, Enhanced salt removal in an inverted capacitive deionization cell using amine modified microporous carbon cathodes, *Environ. Sci. Technol.*, 49 (2015) 10920–10926.
- [9] A. Subramani, J.G. Jacangelo, Emerging desalination technologies for water treatment: A critical review, *Water Res.*, 75 (2015) 164–187.
- [10] M. Biro, D.B. Vončina, Innovative approach to treating waste waters by a membrane capacitive deionisation system, *Chem. Pap.*, 70 (2016) 576–584.
- [11] Y. Liu, C. Nie, X. Liu, X. Xu, Z. Sun, L. Pan, Review on carbon-based composite materials for capacitive deionization, *RSC Adv.*, 5 (2015) 15205–15225.
- [12] K. Laxman, L.A. Gharibi, J. Dutta, Capacitive deionization with asymmetric electrodes: Electrode capacitance vs electrode surface area, *Electrochim. Acta*, 176 (2015) 420–425.
- [13] K. Laxman, M.T.Z. Myint, R. Khan, T. Pervez, J. Dutta, Effect of a semiconductor dielectric coating on the salt adsorption capacity of a porous electrode in a capacitive deionization cell, *Electrochim. Acta*, 166 (2015) 329–337.
- [14] H.-J. Liu, J. Wang, C.-X. Wang, Y.-Y. Xia, Ordered hierarchical mesoporous/microporous carbon derived from mesoporous titanium-carbide/carbon composites and its electrochemical performance in supercapacitor, *Adv. Energy Mater.*, 1 (2011) 1101–1108.
- [15] K.B. Hatzell, M.C. Hatzell, K.M. Cook, M. Boota, G.M. Housel, A. McBride, E.C. Kumbur, Y. Gogotsi, Effect of oxidation of carbon material on suspension electrodes for flow electrode capacitive deionization, *Environ. Sci. Technol.*, 49 (2015) 3040–3047.
- [16] K. Laxman, M.T.Z. Myint, R. Khan, T. Pervez, J. Dutta, Improved desalination by zinc oxide nanorod induced electric field enhancement in capacitive deionization of brackish water, *Desalination*, 359 (2015) 64–70.
- [17] Y. Qu, T.F. Baumann, J.G. Santiago, M. Stadermann, Characterization of resistances of a capacitive deionization system, *Environ. Sci. Technol.*, 49 (2015) 9699–9706.
- [18] K. Sharma, Y.H. Kim, J. Gabitto, R.T. Mayes, S. Yiacoumi, H.Z. Bilheux, L.M.H. Walker, S. Dai, C. Tsouris, Transport of ions in mesoporous carbon electrodes during capacitive deionization of high-salinity solutions, *Langmuir*, 31 (2015) 1038–1047.
- [19] F. Zaera, Probing liquid/solid interfaces at the molecular level, *Chem. Rev.*, 112 (2012) 2920–2986.
- [20] H. Ohshima, *Theory of Colloid and Interfacial Electric Phenomena*, Academic Press, Cambridge, Massachusetts, 2006.
- [21] P.M. Biesheuvel, Y. Fu, M.Z. Bazant, Diffuse charge and Faradaic reactions in porous electrodes, *Phys. Rev. E*, 83 (2011) 061507.
- [22] P.M. Biesheuvel, S. Porada, M. Levi, M.Z. Bazant, Attractive forces in microporous carbon electrodes for capacitive deionization, *J. Solid State Electrochem.*, 18 (2014) 1365–1376.
- [23] P.M. Biesheuvel, M.E. Suss, H.V.M. Hamelers, Theory of water desalination by porous electrodes with fixed chemical charge, arXiv:1506.03948, (2015).
- [24] S. Porada, L. Borchardt, M. Oschatz, M. Bryjak, J.S. Atchison, K.J. Keesman, S. Kaskel, P.M. Biesheuvel, V. Presser, Direct prediction of the desalination performance of porous carbon electrodes for capacitive deionization, *Energy. Environ. Sci.*, 6 (2013) 3700–3712.
- [25] P.M. Biesheuvel, B. van Limpt, A. van der Wal, Dynamic adsorption/desorption process model for capacitive deionization, *J. Phys. Chem. C*, 113 (2009) 5636–5640.
- [26] P.M. Biesheuvel, R. Zhao, S. Porada, A. van der Wal, Theory of membrane capacitive deionization including the effect of the electrode pore space, *J. Colloid Interface Sci.*, 360 (2011) 239–248.
- [27] J.E. Dykstra, R. Zhao, P.M. Biesheuvel, A. van der Wal, Resistance identification and rational process design in capacitive deionization, *Water Res.*, 88 (2016) 358–370.
- [28] B.G. Jeon, H.C. No, Development of a two-dimensional coupled-implicit numerical tool for analysis of the CDI operation, *Desalination*, 288 (2012) 66–71.
- [29] J.-H. Ryu, T.-J. Kim, T.-Y. Lee, I.-B. Lee, A study on modeling and simulation of capacitive deionization process for wastewater treatment, *J. Taiwan Inst. Chem. E.*, 41 (2010) 506–511.
- [30] R. Zhao, P.M. Biesheuvel, H. Miedema, H. Bruning, A. van der Wal, Charge efficiency: a functional tool to probe the double-layer structure inside of porous electrodes and application in the modeling of capacitive deionization, *J. Phys. Chem. Lett.*, 1 (2010) 205–210.
- [31] Y.A.C. Jande, W.S. Kim, Predicting the lowest effluent concentration in capacitive deionization, *Sep. Purif. Technol.*, 115 (2013) 224–230.
- [32] M. Andelman, Flow through capacitor basics, *Sep. Purif. Technol.*, 80 (2011) 262–269.
- [33] T.-Y. Ying, K.-L. Yang, S. Yiacoumi, C. Tsouris, Electrosorption of ions from aqueous solutions by nanostructured carbon aerogel, *J. Colloid Interface Sci.*, 250 (2002) 18–27.
- [34] O.N. Demirer, R.M. Naylor, C.A. Rios Perez, E. Wilkes, C. Hidrovo, Energetic performance optimization of a capacitive deionization system operating with transient cycles and brackish water, *Desalination*, 314 (2013) 130–138.
- [35] L.D. Landau, G. Zito, *Digital Control Systems: Design, Identification and Implementation*, Springer-Verlag, 2006.
- [36] T. Kailath, *Linear Systems*, Prentice Hall, 1980.
- [37] W. Cheney, D. Kincaid, *Numerical Mathematics and Computing*, Brooks-Cole, 2012.
- [38] C. Brasquet, P. Le Cloirec, Effects of activated carbon cloth surface on organic adsorption in aqueous solutions. use of statistical methods to describe mechanisms, *Langmuir*, 15 (1999) 5906–5912.
- [39] J.W. Shim, S.J. Park, S.K. Ryu, Effect of modification with HNO₃ and NaOH on metal adsorption by pitch-based activated carbon fibers, *Carbon*, 39 (2001) 1635–1642.
- [40] J.-H. Lee, W.-S. Bae, J.-H. Choi, Electrode reactions and adsorption/desorption performance related to the applied potential in a capacitive deionization process, *Desalination*, 258 (2010) 159–163.
- [41] C. Wang, H. Song, Q. Zhang, B. Wang, A. Li, Parameter optimization based on capacitive deionization for highly efficient desalination of domestic wastewater biotreated effluent and the fouled electrode regeneration, *Desalination*, 365 (2015) 407–415.